RESEARCH PAPER

Evaluation of Verbascum coromandelianum Constituents by LC-HRMS, Molecular Docking and In-Silico ADMET Analysis for Targeting EGFR Kinase

Saravanakumar Kasimedu[1], Shaik Muskan[2]*

[1] *Seven Hills College of Pharmacy (Autonomous), Venkatramapuram, Tirupati 517561, Andhra Pradesh, India.*
[*2] *Research Scholar, Jawaharlal Nehru Technological University Anantapur, Ananthapuramu – 515002, Andhra Pradesh, India.*

Received: 18th Aug, 2025; Revised: 27th Sep 2025; Accepted: 13th Nov, 2025; Available Online: 30th Nov, 2025

ABSTRACT

The present study aimed to evaluate the phytoconstituents and pharmacological potential of Verbascum coromandelianum through comprehensive physicochemical, phytochemical, LC-HRMS, molecular docking, and in-silico ADMET analyses targeting the Epidermal Growth Factor Receptor (EGFR). The hydroalcoholic extract exhibited characteristic organoleptic properties, acceptable physicochemical parameters, and absence of heavy metals and microbial contaminants, ensuring purity and safety. Preliminary phytochemical screening confirmed the presence of diverse bioactive classes including polyphenols, flavonoids, tannins, fatty acids, and trace alkaloids, suggesting strong therapeutic potential. LC-HRMS profiling identified major compounds such as salidroside, luteolin-7-O-rutinoside, 3,5-di-O-caffeoylquinic acid, oleanolic acid 3-O-glucoside, procyanidin B2 3-O-gallate, pentagalloyl glucose, β-glucogallin, and geraniin. These metabolites are widely associated with antioxidant, anti-inflammatory, hepatoprotective, antidiabetic, cardioprotective, and anticancer activities, validating traditional medicinal applications. Molecular docking revealed strong binding affinities of geraniin (−9.8 kcal/mol), oleanolic acid 3-O-glucoside (−9.7 kcal/mol), pentagalloyl glucose (−9.4 kcal/mol), and luteolin-7-O-rutinoside (−9.2 kcal/mol), surpassing the native EGFR ligand (−8.6 kcal/mol). These compounds formed multiple hydrogen bonds, hydrophobic, and electrostatic interactions with crucial residues, suggesting potential as EGFR inhibitors. In-silico ADMET evaluation indicated favorable drug-likeness, bioavailability, and safety profiles for several compounds, particularly salidroside and β-glucogallin, while polyphenol-rich derivatives exhibited lower toxicity and environmental impact compared to the native ligand. Collectively, the findings highlight Verbascum coromandelianum as a promising source of phytoconstituents with significant therapeutic potential, especially in cancer and oxidative stress-related disorders. Further in vitro and in vivo investigations are warranted to validate these leads and advance formulation development.

Keywords: Verbascum coromandelianum, Hydroalcoholic extract, LC-HRMS analysis, Phytochemical profiling, Computationl analysis, EGFR inhibition.

How to cite this article: Kasimedu S, Muskan S. Evaluation of Verbascum coromandelianum Constituents by LC-HRMS, Molecular Docking and In-Silico ADMET Analysis for Targeting EGFR Kinase. Int J Drug Deliv Technol. 2025;15(4): 1570-1590, DOI: 10.25258/ijddt.15.4.12

Source of support: Nil.

Conflict of interest: None

INTRODUCTION

The Epidermal Growth Factor Receptor (EGFR) is a transmembrane tyrosine kinase receptor that plays a pivotal role in regulating cell growth, differentiation, and survival. Aberrant activation of EGFR signaling is implicated in the pathogenesis of numerous malignancies, including lung, breast, colorectal, and head and neck cancers. Mutations, overexpression, or dysregulated downstream pathways of EGFR contribute to uncontrolled cell proliferation, angiogenesis, and resistance to apoptosis, making EGFR one of the most extensively studied molecular targets in oncology. Several EGFR inhibitors, including tyrosine kinase inhibitors (TKIs) and monoclonal antibodies, have been successfully introduced into clinical practice[1,2,3,4]. However, the therapeutic efficacy of these agents is often compromised by acquired resistance, off-target effects, and toxicity, highlighting the urgent need for safer and more effective alternatives.

Natural products, particularly phytochemicals, offer a promising avenue for the discovery of novel EGFR inhibitors. Phytoconstituents such as flavonoids, phenolic acids, proanthocyanidins, and saponins exhibit structural diversity and bioactivity profiles that enable them to interact with key signaling proteins, including EGFR. Compounds like quercetin, luteolin, and catechins have been reported to inhibit EGFR signaling, demonstrating the therapeutic potential of plant-derived molecules in cancer management[5,6,7]. Importantly, phytochemicals are generally regarded as biocompatible and often exhibit multitargeted mechanisms, reducing the likelihood of resistance development compared with conventional synthetic inhibitors.

**Author for Correspondence: muskanphd798@gmail.com*

To identify such molecules, advanced analytical techniques are indispensable. Liquid Chromatography–High Resolution Mass Spectrometry (LC-HRMS) has emerged as a gold standard for phytochemical profiling due to its high sensitivity, accuracy, and ability to detect a wide spectrum of secondary metabolites[8,9,10,11]. By enabling precise characterization of compounds such as flavonoid glycosides, phenolic acids, tannins, and saponins, LC-HRMS serves as a critical tool for establishing a chemical basis for therapeutic activity. Once identified, these metabolites can be subjected to computational techniques such as molecular docking, which predicts their interaction with EGFR at the molecular level, providing insight into binding affinity and stability. Complementary in-silico ADMET (Absorption, Distribution, Metabolism, Excretion, and Toxicity) modeling further evaluates the pharmacokinetic and safety properties of these compounds, ensuring that only those with favorable drug-like characteristics are prioritized for development[12,13,14,15].

In this context, *Verbascum coromandelianum* (family: Scrophulariaceae), a lesser-explored medicinal plant, presents considerable promise. Traditionally used in South Asian ethnomedicine, this plant has been employed for respiratory ailments, inflammatory conditions, microbial infections, and wound healing. Its therapeutic applications are attributed to a diverse pool of phytochemicals, including phenolic acids, flavonoids, tannins, glycosides, and fatty acids. While other Verbascum species have been studied for their bioactive compounds, V. coromandelianum remains underexplored in terms of systematic phytochemical characterization and target-based pharmacological evaluation. Given the prevalence of polyphenolic compounds in this genus and their known potential for EGFR inhibition, V. coromandelianum warrants detailed investigation.

GRAPHICAL ABSTRACT

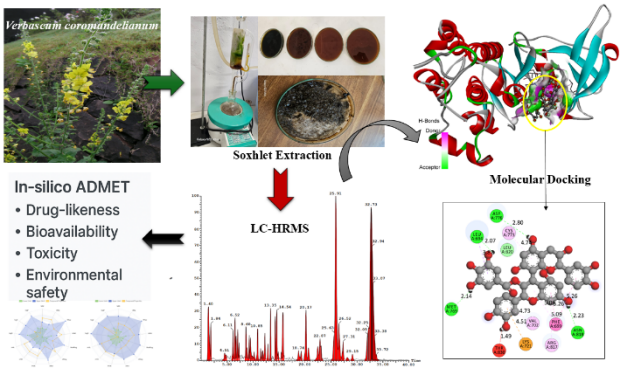

A comprehensive evaluation of this plant involves multiple layers of analysis. First, phytochemical profiling through LC-HRMS provides insight into the diversity of secondary metabolites present in the hydroalcoholic extract. Second, molecular docking studies against EGFR help identify candidate molecules with strong binding affinities and potential inhibitory activity. Third, in-silico ADMET predictions ensure that these candidates exhibit favorable pharmacokinetic behavior and safety, increasing their viability as drug leads. Together, this integrated approach bridges the gap between traditional knowledge and modern drug discovery.

Therefore, the present study was designed to investigate *Verbascum coromandelianum* through LC-HRMS-based phytochemical profiling, followed by molecular docking and in-silico ADMET analysis of its major constituents against EGFR. By combining experimental and computational methodologies, this research aims to uncover bioactive molecules with significant therapeutic potential, provide scientific justification for the traditional use of V. coromandelianum, and contribute to the development of plant-based EGFR inhibitors for cancer management.

MATERIALS AND METHODS

Chemicals and Apparatus

In the present research work, a wide range of analytical grade drugs, chemicals, and reagents were employed. These included crystal iodine, hydrochloric acid, and ethyl acetoacetate obtained from Molychem, Mumbai, while 0.9% sodium chloride was supplied by Avra Chemicals. Other chemicals used comprised dichloromethane, ethyl acetate, n-hexane, ethanol, sodium hydroxide, Folin–Ciocalteu reagent, phenazine methosulfate, ferric chloride, acetone, carbon tetrachloride, potassium hydroxide, benzene, benzaldehyde, nicotinamide adenine dinucleotide, sodium nitroprusside, trichloroacetic acid, thiobarbituric acid, L-ascorbic acid, napthaldehyde, magnesium chloride, and potassium chloride.

For experimental procedures, both general laboratory glassware and specialized instruments were utilized. Apparatus included Soxhlet's extractor (Lab Trading Laboratory, Aurangabad), separating funnels, round bottom flasks, test tubes, reflux assemblies, glass rods, conical flasks, funnels, TLC plates, capillaries, beakers, and precoated aluminum silica gel plates (E. Merck, Germany). Essential instruments comprised a rotary evaporator (Buchi, Switzerland), heating mantle (TOPLAB, India), magnetic stirrer (Remi), and a digital melting point apparatus (SESW). Together, these chemicals and instruments supported the successful execution of phytochemical and analytical investigations.

Collection of Plant Material and Authentication

The whole plant of *Verbascum coromandelianum* (Vahl.), belonging to the family Scrophulariaceae, was collected during December 2024 from the local region of Buldhana, Maharashtra, India. An herbarium specimen was prepared and submitted for authentication to the Department of Botany, Sri Venkateswara University, Tirupati, Andhra Pradesh. The plant material was taxonomically identified and authenticated by Dr. K. Madhava Chetty, Plant Taxonomist, Retd. Assistant Professor, Department of Botany, Sri Venkateswara University. The authenticated specimen was assigned the voucher number 0787. Following authentication and certificate issuance, the plant material was processed further for extraction and experimental analysis.

Soxhlet Extraction with Hydroalcoholic Solvent

Leaves and bark of *Verbascum coromandelianum* were collected, thoroughly washed with distilled water, and shade-dried at room temperature for one week to prevent

loss of volatile constituents. The dried material (500 g) was coarsely powdered and extracted using a Soxhlet apparatus with a hydroalcoholic solvent mixture (ethanol:water, 70:30). Extraction was carried out for about 24 hours with multiple siphon cycles, indicated by the dark green color of the solvent in the flask and the fading color of the plant material. The obtained extract was concentrated by natural solvent evaporation in Petri plates and subsequently used for qualitative phytochemical analysis[16,17,18,19]. The working photographs of Soxhlet extraction are depicted in Figure 1.

Figure 1. The Soxhlet extraction of Verbascum coromandelianum

Physicochemical Analysis

The extract was subjected to various physicochemical evaluations. Its colour, odour, and taste were examined under natural light and by sensory testing. The pH values of 1% and 10% aqueous solutions were measured using a digital pH meter for accuracy. The foreign matter content was determined by separating and weighing extraneous material, while the loss on drying (LOD) was assessed at 105 °C until a constant weight was achieved[20,21].

Ash values were estimated to determine the inorganic content: total ash by incineration, acid-insoluble ash with dilute hydrochloric acid, sulphated ash after treatment with sulphuric acid at high temperature, and water-soluble ash by boiling in water and weighing the insoluble fraction. Extractive values were determined for alcohol- and water-soluble components by macerating powdered drug samples with respective solvents, followed by filtration, evaporation, and calculation of percentage yield.

To ensure safety, heavy metal content (As, Cd, Pb, Hg, Zn, Cu, Cr, Mn) was analyzed using atomic absorption spectrophotometry after microwave digestion with nitric acid, following standard operating conditions[22]. Each sample was tested in triplicate and compared with standard solutions. Similarly, pesticide residues were assessed by concentrating extracts, passing them through a clean-up column, and analyzing by gas chromatography with an electron capture detector. The method ensured high sensitivity (0.1–0.5 ppb), with recovery rates above 80%, and external standards were used for validation[23].

Preliminary Phytochemical and Microbial Evaluation

The extract was analyzed for major phytoconstituents using standard qualitative assays. Tests confirmed the presence of carbohydrates, proteins, amino acids, fixed oils, steroids, glycosides, flavonoids, alkaloids, tannins, phenolics, and saponins, indicating rich phytochemical diversity [20,21,24].

Microbial quality was assessed through serial dilutions and culture on nutrient agar, MacConkey agar, cetrimide agar, and Sabouraud dextrose agar, followed by incubation at suitable conditions for bacterial and fungal growth. Colony counts were expressed as CFU per gram or milliliter. Specific contamination tests were performed for *Escherichia coli*, *Salmonella* spp., *Shigella* spp., *Pseudomonas aeruginosa*, and *Staphylococcus aureus* using enrichment media, selective agar plates, and confirmatory biochemical assays[25,26.]

LC-HRMS Analysis

Liquid chromatography–high resolution mass spectrometry (LC-HRMS) analysis was performed using an Accucore™ C18 column (150 × 4.6 mm, 2.6 µm particle size). The separation was achieved under reversed-phase conditions with a programmed gradient elution system. A defined volume of each sample was injected into the column, and the eluent was continuously monitored by an integrated UV detector. The mass spectrometer was operated with electrospray ionization (ESI) in both positive and negative modes. Instrumental parameters including source temperature, desolvation gas flow, and capillary voltage were optimized to ensure stable ion generation and reproducibility. Data were collected in centroid mode across a broad mass-to-charge (m/z) range, and chromatographic as well as spectral data were recorded simultaneously. All analyses were performed under controlled laboratory conditions, and instrument software was used to process raw data, ensuring accurate acquisition of retention times and high-resolution mass spectra for subsequent compound characterization[27,28,29.]

Molecular Docking

Molecular docking studies were conducted to evaluate the binding interactions between the phytoconstituents identified from *Verbascum coromandelianum* and the target protein Epidermal Growth Factor Receptor (EGFR), using the crystal structure with PDB ID: 4JQ7 (Figure 2). Initially, the 3D structures of identified compounds were sketched using ChemDraw and converted to 3D SDF format using Chem3D. These ligands were retrieved and optimized for docking by performing energy minimization using Open Babel integrated within PyRx software.

The 3D crystal structure of EGFR (PDB ID: 4JQ7) was obtained from the RCSB Protein Data Bank. Before docking, the protein was prepared using Discovery Studio Visualizer by removing water molecules, co-crystallized ligands, and heteroatoms. Polar hydrogens were added, and Kollman charges were assigned using AutoDock tools integrated within PyRx. The active site of the EGFR receptor was defined based on literature and confirmed using Discovery Studio, with grid box parameters centered at coordinates X: -51.846290, Y: -0.213097, Z: -22.521000. The grid box was adjusted to cover the entire active site pocket. Docking simulations were performed using AutoDock Vina embedded in PyRx. Each ligand was docked individually into the defined binding site, and the best binding conformations were selected based on the lowest binding affinity (in kcal/mol). The resulting docked complexes were visualized and analyzed for molecular interactions (hydrogen bonding, hydrophobic interactions, π–π stacking, etc.) using Discovery Studio Visualizer. Native ligand interactions from the 4JQ7 structure were also used as a comparative reference to evaluate the efficacy of the phytoconstituents [12–15].

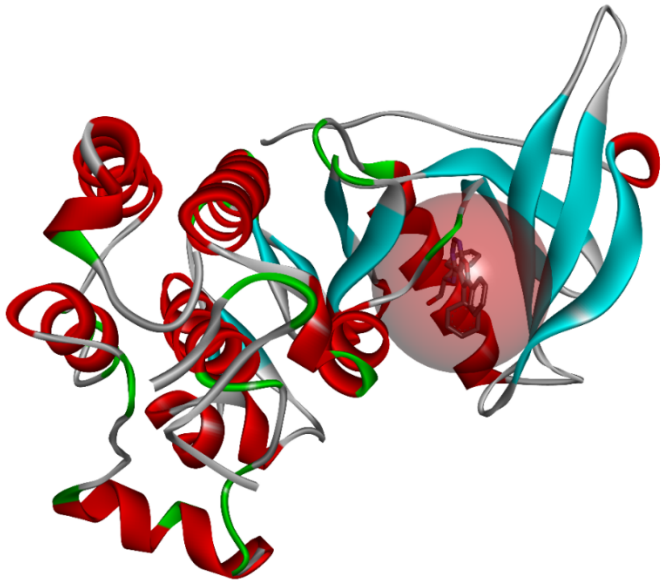

Figure 2. Active cavity of EGFR enzyme (PDB ID: 4JQ7) with native ligand.

***In silico* ADMET analysis**

In-silico ADMET (Absorption, Distribution, Metabolism, Excretion, and Toxicity) analysis was conducted to evaluate the pharmacokinetic and toxicity profiles of the phytoconstituents identified from *Verbascum coromandelianum*. The 2D structures of compounds were drawn using ChemDraw and converted to SMILES format via Chem3D. These SMILES were then input into online tools SwissADME (https://admetlab3.scbdd.com/server/evaluation) and ADMETlab 3.0 (https://admetmesh.scbdd.com/) for prediction of drug-likeness, gastrointestinal absorption, blood-brain barrier permeability, cytochrome P450 inhibition, and potential toxicity. The results were interpreted to assess the suitability of each compound as a drug-like candidate targeting EGFR [12–15].

RESULTS AND DISCUSSIONS

Organoleptic and Physicochemical Analysis of Extracts

The hydroalcoholic extract of *Verbascum coromandelianum* was prepared and assessed for its organoleptic and physicochemical characteristics (Table 1). The extract appeared dark brown to greenish-brown with a herbaceous to mildly aromatic odour and a distinctly bitter–astringent taste, features often associated with phenolic- and flavonoid-rich botanicals. Its texture was solid to sticky, and the yield of extraction was 12.4%, indicating moderate recovery of active constituents. Physicochemical analysis showed a near-neutral pH of 6.9 in 1% solution and

a slightly acidic pH of 6.1 in 10% solution, both acceptable for oral and topical use. The sample was devoid of foreign matter and heavy metals, confirming purity and safety. Moisture content, measured as loss on drying, was 5.21%, suggesting good storage stability. Ash values, reflective of mineral and inorganic content, were within pharmacopoeial standards with total ash at 14.15%, acid-insoluble ash at 2.55%, water-soluble ash at 8.75%, and sulphated ash at 4.32%. Extractive values indicated higher alcohol solubility (16.88%) compared with water solubility (15.51%), pointing to the presence of moderately polar constituents such as flavonoids, alkaloids, and fatty acids.

Table 1. The physicochemical analysis of Verbascum coromandelianum extract

Parameters	**Observation**
pH	
1% Solution	6.9
10% Solution	6.1
Foreign content	0%
LOD	5.21%
Ash values	
Total Ash value	14.15%
Acid insoluble ash value	2.55%
Water soluble ash value	8.75%
Sulphated ash value	4.32%
Extractive values	
Alcohol-soluble extractive	16.88%
Water-soluble extractive	15.51%
Heavy metals estimation (present)	Absent
Pesticide residues	Absent

Preliminary Phytochemical Screening and Microbial Evaluation

Preliminary phytochemical screening of the extract revealed the presence of several secondary metabolites responsible for its therapeutic potential (Figure 3). Carbohydrates were detected in trace amounts, while reducing sugars and monosaccharides showed uncertain responses. Proteins and amino acids were moderately present, suggesting the presence of simple peptides and derivatives. A notable feature was the abundant presence of fats and oils, which can be attributed to fatty acids such as palmitic and oleic acid. Steroids were detected in low concentrations, whereas cardiac glycosides and saponins gave inconclusive results, and anthraquinone glycosides were absent. Trace amounts of alkaloids were observed, along with abundant phenolic compounds and flavonoids, which included phenols, benzoic acid derivatives, and chromanone-type flavonoids. Tannins were also present in low levels. The overall phytochemical profile, particularly the richness in polyphenols and flavonoids, underpins the plant's traditional use in managing inflammatory, oxidative stress-related, and microbial disorders.

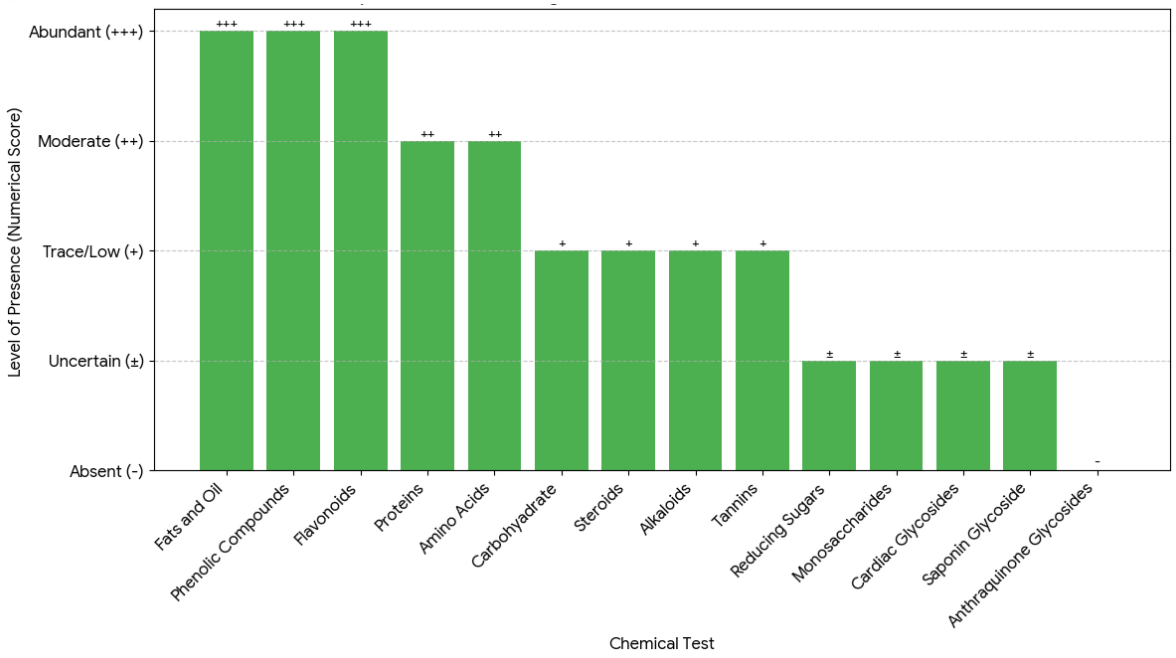

Figure 3. The results of preliminary phytochemical screening of *Verbascum coromandelianum* extract.

Microbial analysis of the hydroalcoholic extract of *Verbascum coromandelianum* confirmed its microbiological safety. The extract was free from common pathogenic organisms such as Escherichia coli, Salmonella spp., Shigella spp., Pseudomonas aeruginosa, and Staphylococcus aureus, indicating compliance with quality standards and suggesting that appropriate handling and preparation practices were maintained. The absence of these contaminants supports its suitability for subsequent pharmacological testing and formulation development

LC-HRMS analysis

The LC-HRMS analysis of the hydroalcoholic extract (*Verbascum coromandelianum*) revealed a wide spectrum of secondary metabolites, with peaks corresponding to phenolic glycosides, flavonoids, caffeoylquinic acids, saponins, proanthocyanidins, gallotannins, and ellagitannins (Figure 4). Identification was based on accurate mass (m/z), retention time (RT), and fragmentation pattern analysis compared with literature and reference databases.

At RT 1.38 min, a compound tentatively identified as salidroside (phenolic glycoside) was detected. The presence of sugar-related fragments (m/z 543.2) alongside a phenolic core (m/z 365.1) confirms the glycosidic nature of the molecule. Phenolic glycosides are known for their antioxidant, anti-fatigue, and neuroprotective effects, suggesting a potential role in cytoprotective activity. At RT 1.83 min, a flavonoid glycoside (luteolin-7-O-rutinoside) was observed with a molecular ion at m/z 705.2 and characteristic flavonoid fragments. Luteolin derivatives are extensively reported for their anti-inflammatory, antidiabetic, and hepatoprotective roles, making this compound highly significant in pharmacological contexts. The peak at RT 4.69 min was assigned to 3,5-di-O-caffeoylquinic acid, a well-known chlorogenic acid derivative. Its diagnostic ion at m/z 329.1 and supporting fragments (m/z 463.1) confirm the caffeoylquinic acid backbone. Such compounds exhibit strong antioxidant, antimutagenic, and cardioprotective properties, which may enhance the therapeutic potential of the extract. At RT 6.50 min, a triterpenoid saponin (oleanolic acid 3-O-glucoside) was detected, as indicated by the base ion m/z 293.1 and higher sugar-linked fragments (>600 m/z). Saponins are amphiphilic compounds with diverse biological activities, including cholesterol-lowering, immunomodulatory, and anticancer effects. A significant peak at RT 10.87 min corresponded to procyanidin B2 3-O-gallate, a proanthocyanidin dimer. The high molecular ion (m/z 1006.5) and characteristic catechin/epicatechin fragments (m/z 329.1, 512.2) support its identification. Proanthocyanidins are well-documented for their antioxidant, cardioprotective, antimicrobial, and anticancer activities. The peak at RT 11.83 min indicated the presence of pentagalloyl glucose, a high-molecular-weight gallotannin. Its intense polyphenolic fragmentation (m/z 698.4, 549.2, 320.2) confirms its tannin structure. Pentagalloyl glucose has been studied for its antitumor, antiviral, and hepatoprotective actions, highlighting its pharmacological significance. At RT 14.56 min, a glycosylated polyphenol (β-glucogallin) was detected, characterized by very high m/z values (1073.8, 1075.7). This compound is a known precursor of hydrolyzable tannins and contributes to antioxidant and anti-inflammatory activities. Finally, the late-eluting compound at RT 25.41 min was identified as geraniin (ellagitannin derivative) with a molecular ion at m/z 1290.7. Ellagitannins are reported to possess antioxidant, antiviral, antibacterial, and hepatoprotective properties, and their strong interaction with the C18 column explains the long retention time.

Overall, the LC-HRMS profile of the sample highlights the dominance of polyphenolic compounds, flavonoids, and tannins, supported by the detection of saponins and glycosides. These metabolites are well-recognized for their broad spectrum of biological activities, including antioxidant, anti-inflammatory, antidiabetic, hepatoprotective, cardioprotective, and anticancer effects. The results align with the traditional medicinal use of polyphenol- and saponin-rich plants and provide a chemical basis for the bioactivity of the extract.

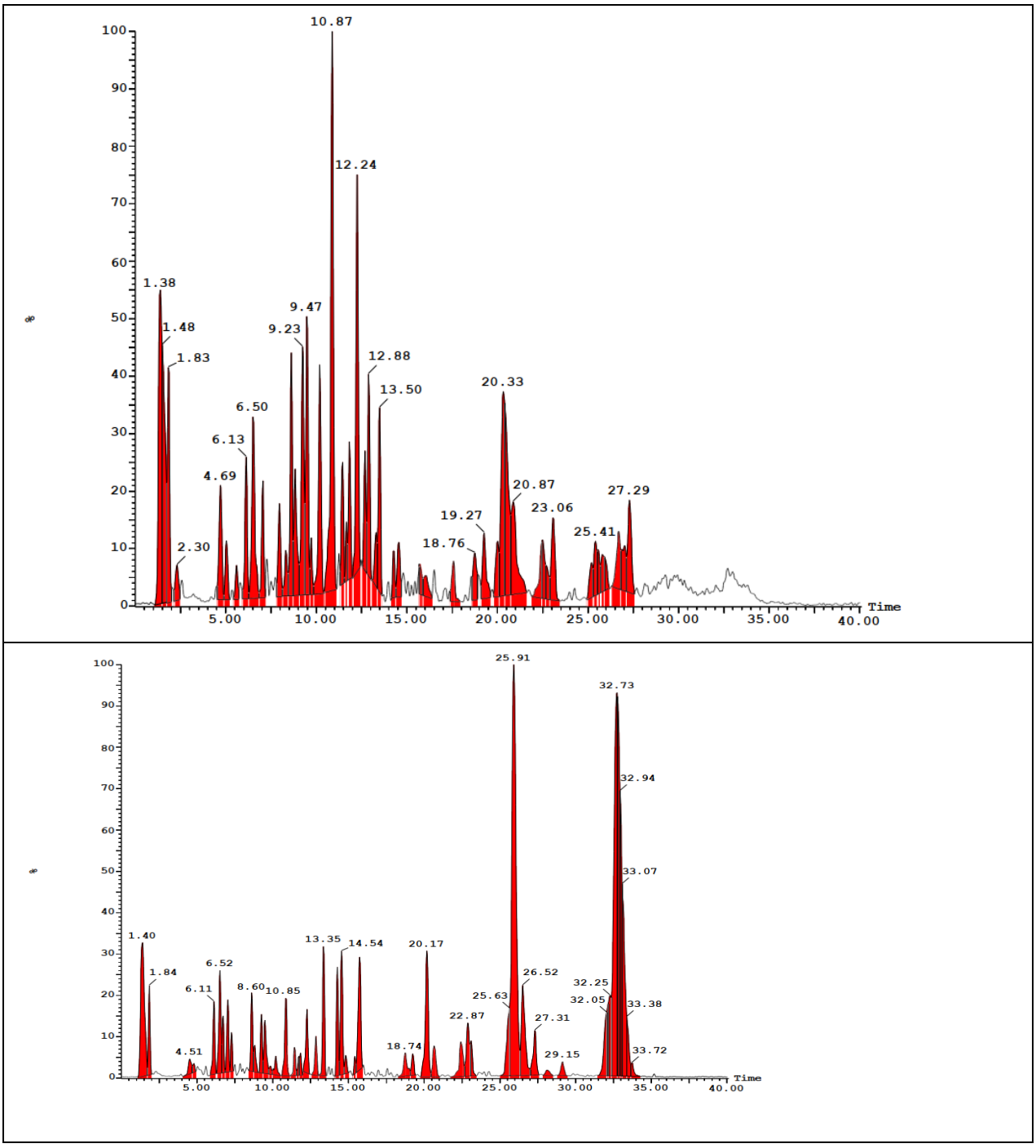
10.87
12.24
1.38
1.48
1.83
9.47
9.23
12.88
13.50
20.33
6.50
6.13
4.69
20.87
23.06
27.29
19.27
18.76
25.41
2.30
Time
25.91
32.73
32.94
33.07
1.40
1.84
6.52
6.11
8.60
10.85
13.35
14.54
20.17
26.52
25.63
22.87
32.25
32.05
33.38
27.31
4.51
18.74
29.15
33.72
Time

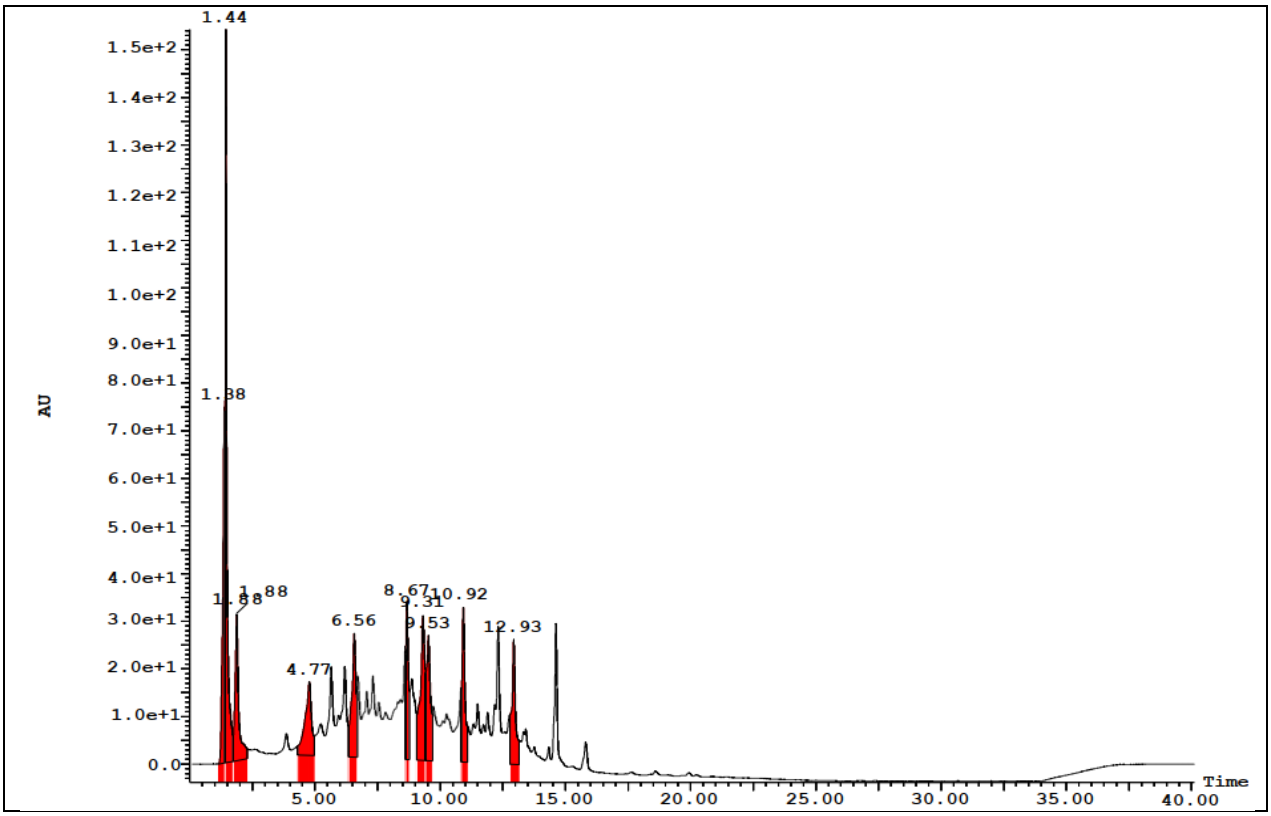

Figure 4. LC-HRMS graph of *Verbascum coromandelianum*

Molecular Docking

The molecular docking analysis of selected constituents from *Verbascum coromandelianum* against the EGFR enzyme (PDB ID: 4JQ7) demonstrated promising interactions, with several compounds exhibiting stronger binding affinities compared to the native ligand, which had a binding energy of -8.6 kcal/mol (Table 2). The native ligand interacted primarily through a hydrogen bond with MET769, hydrophobic interactions with LEU820 and VAL702, and other interactions including Pi-Sulfur with MET742. However, it showed limited hydrogen bonding and electrostatic interactions, which may contribute to its relatively lower binding affinity. Among the tested phytoconstituents, Geraniin exhibited the most favorable binding affinity of -9.8 kcal/mol, significantly surpassing the native ligand. It formed multiple conventional hydrogen bonds with ASP831, GLU738, ASP813, and THR830, along with Pi-Anion electrostatic interactions with ASP776. Additionally, its interactions with key residues such as LEU820 (Pi-Sigma), PHE699 (Pi-Pi stacked), and LEU694 (Amide-Pi stacked) suggest a robust and stable binding mode within the EGFR active site. Oleanolic acid 3-O-glucoside also showed strong binding energy (-9.7 kcal/mol), characterized by conventional hydrogen bonding with SER696 and extensive hydrophobic interactions including Pi-Alkyl and Alkyl interactions with LEU820, VAL702, and ALA719. These interactions support its high binding potential, indicating effective accommodation within the EGFR binding pocket.

Similarly, Pentagalloyl glucose demonstrated a high binding affinity of -9.4 kcal/mol. It engaged in multiple hydrogen bonds with LEU764, PRO770, ASP813, and CYS773, along with electrostatic interactions (Pi-Cation with LYS721 and Pi-Anion with ASP831). Its π-stacking with PHE699 and Pi-Alkyl interaction with ALA719 further support its strong stabilization within the binding site. Luteolin-7-O-rutinoside exhibited a binding affinity of -9.2 kcal/mol and formed several hydrogen bonds with ASP831, LYS721, and MET769. It also showed hydrophobic interactions, particularly Pi-Sigma and Pi-Alkyl types with LEU694 and VAL702. These interactions suggest good compatibility with EGFR's active residues, enhancing its binding affinity over the native ligand.

Procyanidin B2 3-O-gallate also displayed a notable binding energy of -9.1 kcal/mol. It formed hydrogen bonds with ASP776, LEU694, MET769, and ASN818, and showed π-based interactions such as Pi-Sigma and Pi-Pi stacking with LEU694 and PHE699. Its capacity to engage in both hydrogen bonding and hydrophobic interactions underscores its inhibitory potential. 3,5-Di-O-caffeoylquinic acid recorded a binding affinity of -9.0 kcal/mol, forming conventional hydrogen bonds with LYS721 and MET769, and electrostatic Pi-Anion interaction with ASP831. Additionally, Pi-Sigma interaction with LEU694 and Pi-Pi stacking with PHE699 contributed to its stabilized binding, slightly better than the native ligand.

Beta-Glucogallin and Salidroside, on the other hand, showed lower binding affinities (-7.7 and -7.4 kcal/mol, respectively), weaker than the native ligand. Though they engaged in hydrogen bonding and some electrostatic and hydrophobic interactions, the lower energy values and fewer high-affinity interactions suggest weaker binding efficacy. In summary, compounds such as Geraniin,

Oleanolic acid 3-O-glucoside, Pentagalloyl glucose, and Luteolin-7-O-rutinoside not only outperformed the native ligand in terms of binding affinity but also exhibited diverse and stable interaction profiles with crucial EGFR active site residues. Their ability to form strong hydrogen bonds, electrostatic interactions, and π-based stacking provides a molecular basis for their potential as EGFR inhibitors. These findings justify further in-depth in vitro and in vivo evaluations of these phytoconstituents for anticancer drug development.

Table 2. Binding interactions of selected compounds and native ligand with EGFR enzyme (PDBID: 4JQ7).

Amino acid residues	Bond Length	Bond Type	Bond Category	Ligand Energy (Kcal/mol)	Binding Affinity
Native Ligand					
MET769	3.33419	Hydrogen Bond	Carbon Hydrogen Bond	720.92	-8.6
LEU820	3.75236	Hydrophobic	Pi-Sigma		
MET742	5.32119	Other	Pi-Sulfur		
VAL702	4.75191	Hydrophobic	Pi-Alkyl		
ALA719	4.14641				
CYS773	4.96353				
VAL702	5.44838				
ALA719	4.74199				
LYS721	4.65064				
3,5-Di-O-caffeoylquinic acid					
LYS721	2.76932	Hydrogen Bond	Conventional Hydrogen Bond	297.06	-9
LYS721	2.98039				
MET769	2.09411				
ASP831	3.44674	Electrostatic	Pi-Anion		
LEU694	3.70415	Hydrophobic	Pi-Sigma		
PHE699	4.36654		Pi-Pi Stacked		
beta-Glucogallin					
ASP831	2.516	Hydrogen Bond	Conventional Hydrogen Bond	657.32	-7.7
LEU764	2.97624				
GLU738	2.49959				
THR766	1.8806				
LYS721	4.59214	Electrostatic	Pi-Cation		
LEU694	3.9584	Hydrophobic	Pi-Sigma		
VAL702	5.33394		Pi-Alkyl		
ALA719	5.44725				
LYS721	4.47085				
VAL702	5.38497				
ALA719	5.14848				
LEU820	5.15569				
Geraniin					
ASP831	2.21829	Hydrogen Bond	Conventional Hydrogen Bond	1300.72	-9.8
GLU738	2.88681				
ASP813	1.95109				
THR830	2.46638				
ASP776	3.48231	Electrostatic	Pi-Anion		
ASP831	2.99246				
LEU820	3.42303	Hydrophobic	Pi-Sigma		
PHE699	4.89054		Pi-Pi Stacked		
LEU694	4.47806		Amide-Pi Stacked		
CYS773	4.24521		Alkyl		
LEU694	5.32331		Pi-Alkyl		
VAL702	5.43637				
VAL702	5.489				
PHE699	4.10577				
Luteolin-7-O-rutinoside					
ASP831	2.59633			416.27	-9.2

ASP831	1.86526	Hydrogen Bond	Conventional Hydrogen Bond		
LYS721	2.52436				
MET769	1.90742				
LEU694	3.66529	Hydrophobic	Pi-Sigma		
LEU694	5.36286		Pi-Alkyl		
VAL702	4.8553				
ALA719	4.32778				
LEU820	4.85644				
VAL702	5.07512				
ALA719	5.31534				
LYS721	4.82924				
Oleanolic acid 3-O-glucoside					
SER696	2.11857	Hydrogen Bond	Conventional Hydrogen Bond	713.66	-9.7
ALA719	3.29649		Carbon Hydrogen Bond		
LEU820	3.83595	Hydrophobic	Alkyl		
LEU694	4.5777				
VAL702	3.82425				
ALA719	3.96813				
VAL702	4.3392				
CYS773	4.72323				
LEU820	4.43609				
VAL702	4.39208				
LEU820	5.03699				
PHE699	5.46995		Pi-Alkyl		
Pentagalloyl glucose					
LEU764	2.61092	Hydrogen Bond	Conventional Hydrogen Bond	476.85	-9.4
PRO770	2.55467				
LEU694	1.82672				
ASP813	2.70486				
LYS721	2.08293				
CYS773	2.32699				
ASN818	2.42907				
LYS721	4.8555	Electrostatic	Pi-Cation		
ASP831	3.44127		Pi-Anion		
LEU694	3.71929	Hydrophobic	Pi-Sigma		
CYS773	5.09919	Other	Pi-Sulfur		
PHE699	4.79385	Hydrophobic	Pi-Pi Stacked		
ALA719	5.0595		Pi-Alkyl		
LYS721	4.01767				
ARG817	4.78399				
PHE699	5.12932				
Procyanidin B2 3-O-gallate					
ASP776	2.79589	Hydrogen Bond	Conventional Hydrogen Bond	526.84	-9.1
LEU694	2.07113				
MET769	2.13777				
ASN818	2.22687				
LYS721	4.51125	Electrostatic	Pi-Cation		
LEU694	3.86842	Hydrophobic	Pi-Sigma		
PHE699	5.25974		Pi-Pi Stacked		
PHE699	5.26024		Pi-Pi T-shaped		
ARG817	5.09399		Pi-Alkyl		
CYS773	4.74032				
VAL702	4.73325				
LYS721	4.79272				
PHE699	5.06186				
Salidroside					
MET769	2.30735			670.48	-7.4

ALA719	2.59716	Hydrogen Bond	Conventional Hydrogen Bond		
LEU764	2.19322				
THR766	2.26006				
LYS721	4.47696	Electrostatic	Pi-Cation		
LEU694	3.58755	Hydrophobic	Pi-Sigma		
MET742	5.78413	Other	Pi-Sulfur		
VAL702	5.18187	Hydrophobic	Pi-Alkyl		
ALA719	5.46998				
LYS721	4.31774				
ALA719	5.42168				

Table 3. 2D and 3D binding interaction poses of selected derivatives with EGFR enzyme.

3D Binding Poses	**2D Binding Poses**
Native Ligand	
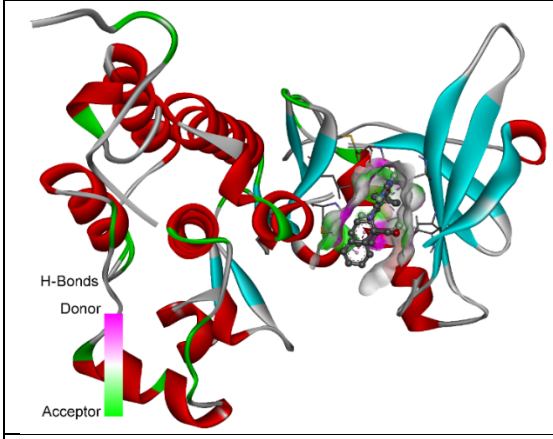	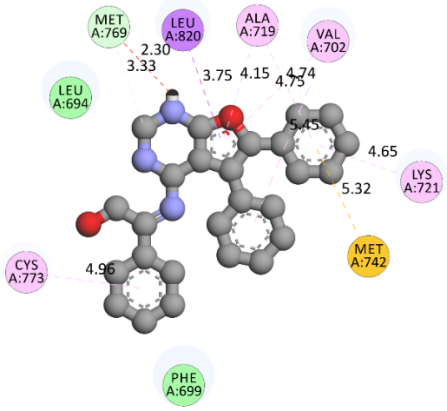
3,5-Di-O-caffeoylquinic acid	
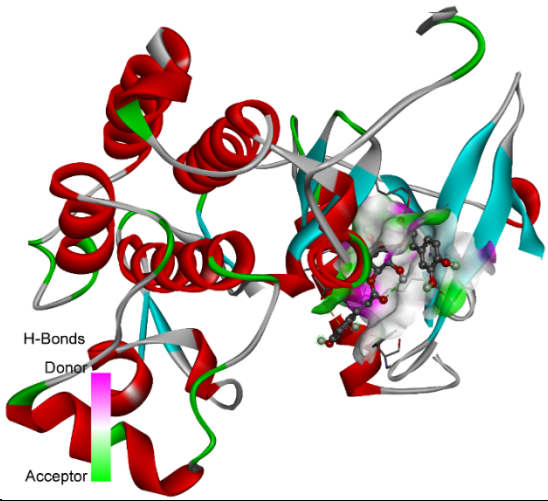	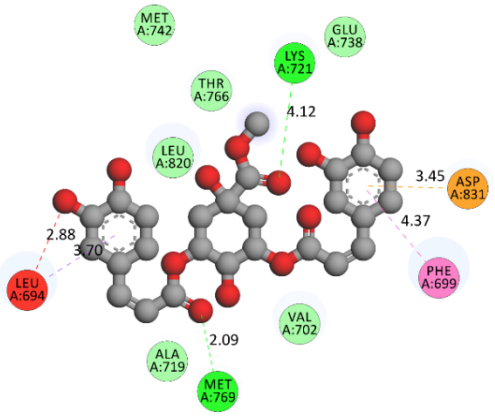
beta-Glucogallin	

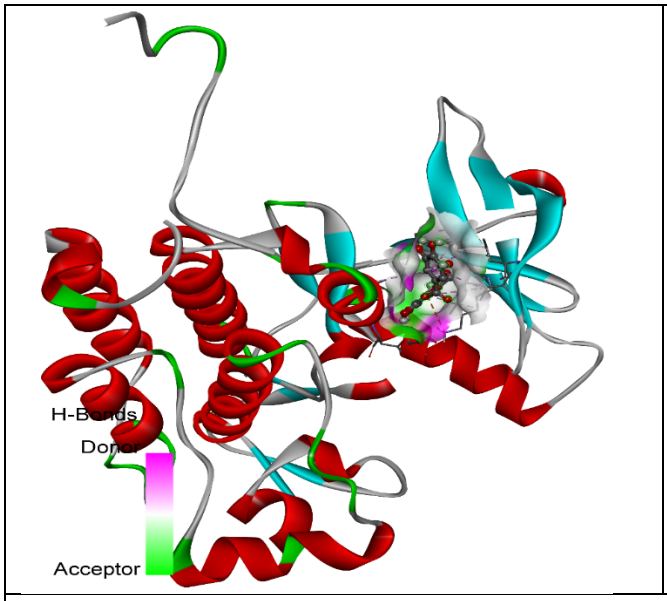

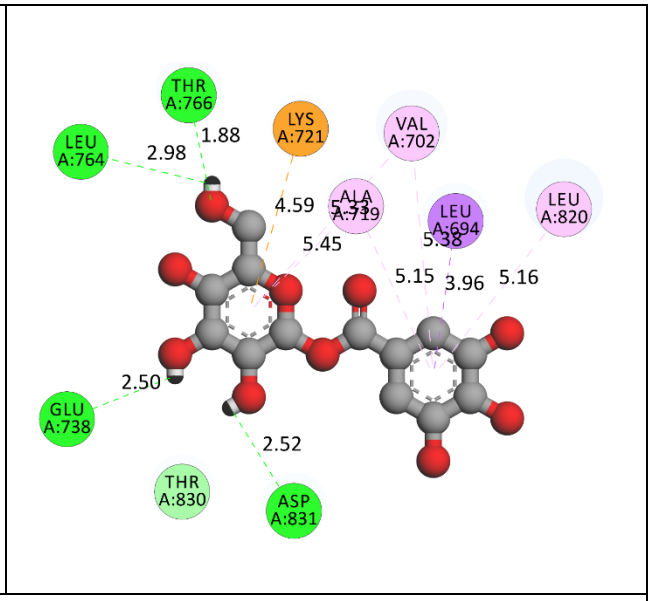

Geraniin

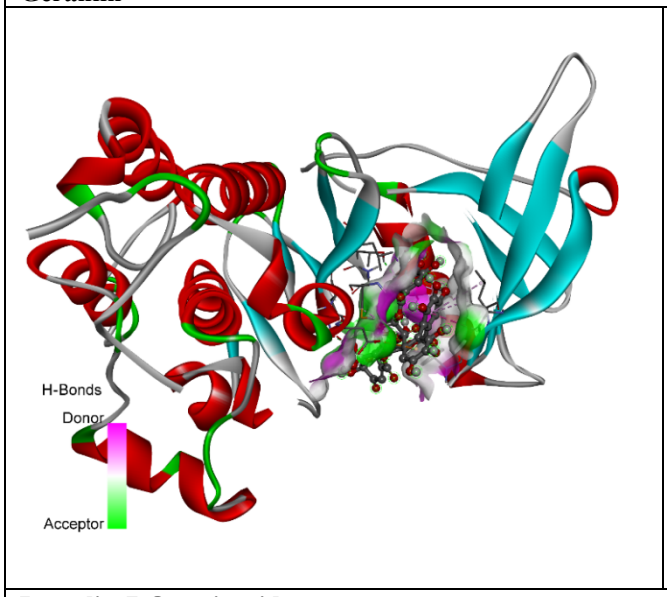

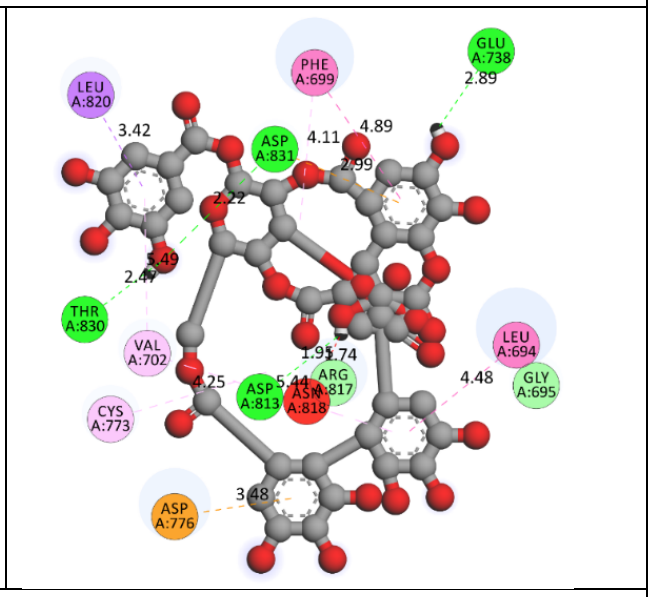

Luteolin-7-O-rutinoside

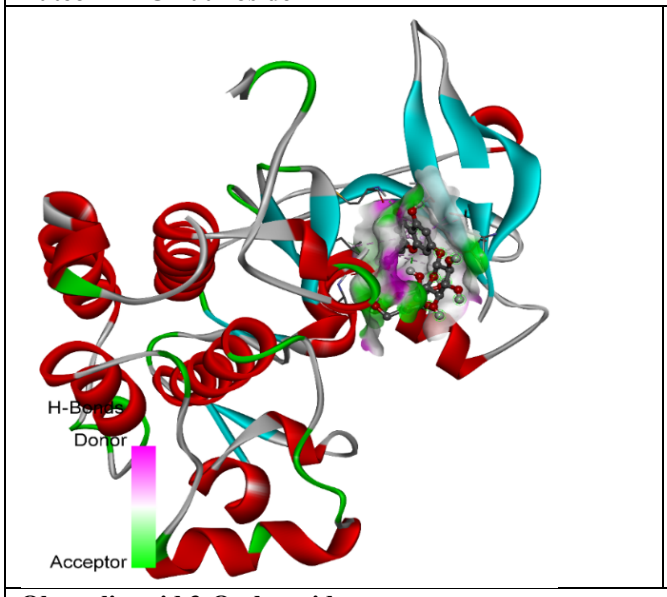

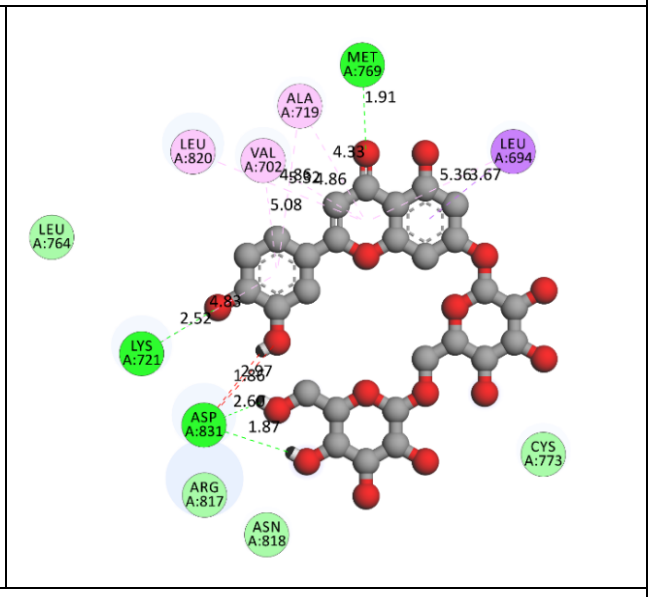

Oleanolic acid 3-O-glucoside

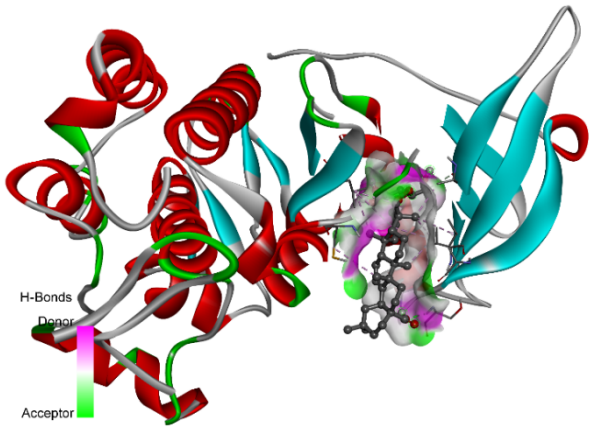

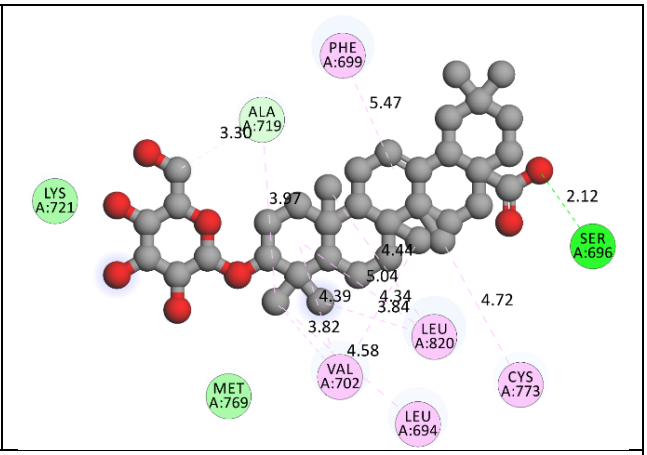

Pentagalloyl glucose

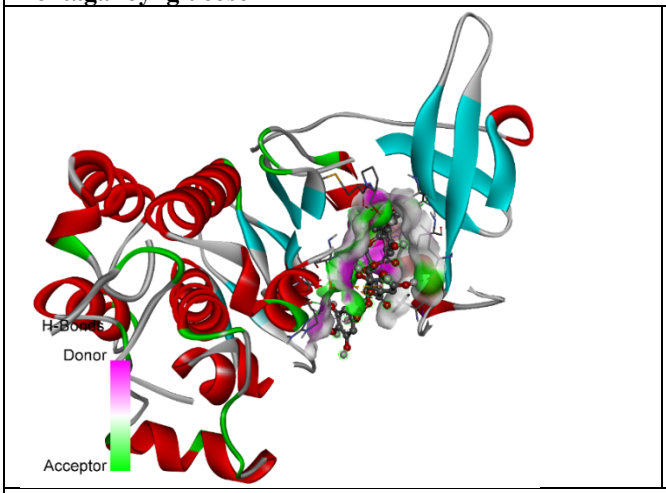

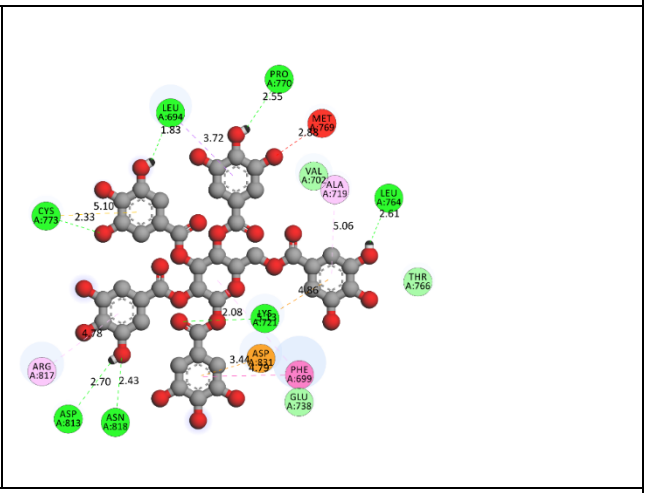

Procyanidin B2 3-O-gallate

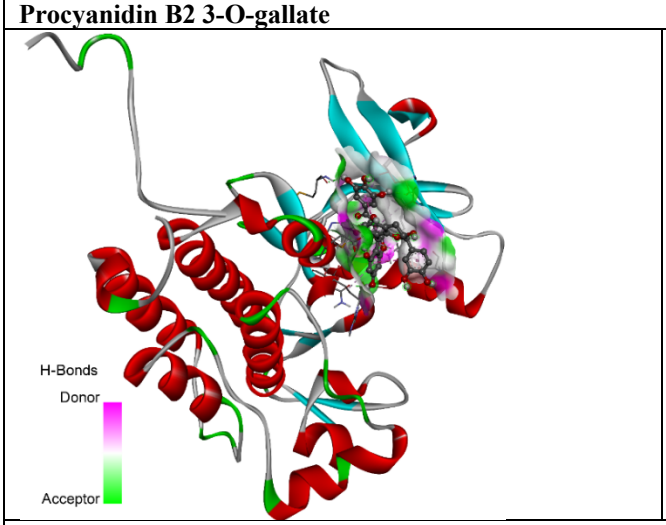

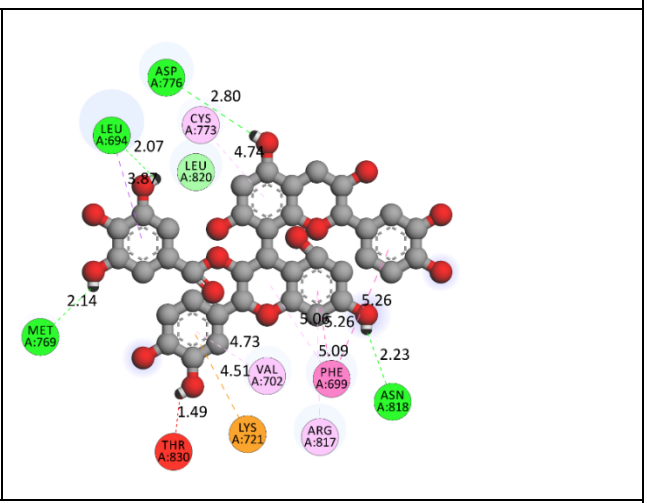

Salidroside

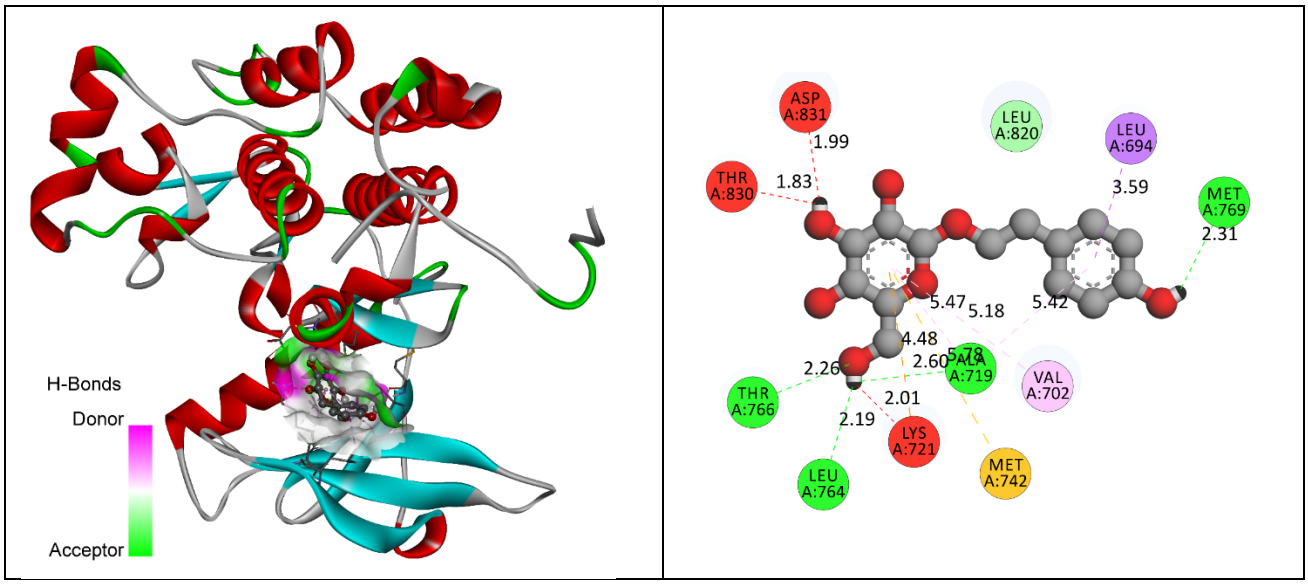

***In silico* ADMET analysis**

Table 4 presents the physicochemical characteristics of selected *Verbascum coromandelianum* constituents and the native ligand. Native ligand has a moderate molecular weight (MW = 407.16) and low polarity (TPSA = 71.18), whereas most plant-derived molecules, like Geraniin (MW = 952.08, TPSA = 450.25) and Pentagalloyl glucose (MW = 940.12, TPSA = 444.18), are heavier and more polar, indicating reduced membrane permeability. Beta-Glucogallin and Salidroside, with moderate MWs (332.07 and 300.12 respectively) and favorable logP values (−1.23 and −0.57), display better hydrophilic–lipophilic balance compared to Native Ligand (logP = 4.28), suggesting higher solubility. Native ligand is more lipophilic, but many plant compounds exhibit superior TPSA and lower logP, which may benefit oral absorption. LogS values also show that compounds like beta-Glucogallin (logS = −1.09) and Salidroside (logS = −1.35) have better solubility than the native ligand (logS = −4.52). Hence, several natural derivatives demonstrate drug-like physicochemical profiles suitable for oral delivery.

As shown in Table 5, drug-likeness properties of selected compounds were assessed using various predictive rules. The native ligand shows moderate QED (0.378) and fails the Lipinski rule but adheres to Pfizer and GSK rules. In contrast, Salidroside displays the highest QED (0.461), indicating strong drug-likeness potential, and complies with all tested rules. Beta-Glucogallin and Oleanolic acid 3-O-glucoside also show acceptable profiles, although their QED scores (0.236 and 0.218, respectively) are lower. Many compounds, including Geraniin, Luteolin-7-O-rutinoside, and Pentagalloyl glucose, violate the Lipinski rule, which could limit bioavailability. The chelator rule is triggered for polyphenolic-rich compounds like 3,5-Di-O-caffeoylquinic acid, suggesting metal-binding potential, possibly impacting bioactivity. Overall, while native ligand presents limited rule compliance, compounds like Salidroside and beta-Glucogallin stand out for balanced drug-likeness, making them promising candidates for further optimization.

Table 6 evaluates absorption-related metrics including Caco-2 and MDCK permeability, P-glycoprotein interaction, and oral bioavailability. Native ligand shows relatively high permeability (Caco-2 = −4.58), suggesting moderate intestinal uptake. Most phytocompounds exhibit poorer permeability, with Geraniin (−7.17) and Pentagalloyl glucose (−8.02) being the least permeable. However, these same molecules exhibit excellent predicted oral bioavailability (F30% and F50% > 0.99), likely due to other transport mechanisms. Notably, Salidroside shows the best balance—moderate permeability, strong P-gp substrate affinity, and high oral bioavailability (F50% = 0.99). native ligand is a strong P-gp inhibitor (0.911), potentially increasing drug–drug interactions. Compounds such as Luteolin-7-O-rutinoside and Procyanidin B2 3-O-gallate also exhibit favorable absorption profiles. Thus, while native ligand outperforms in permeability, several natural candidates offer better bioavailability, suggesting their suitability for oral formulation with proper delivery systems.

Distribution and metabolic profiles (Table 7) reveal notable differences between natural constituents and native ligand. The native ligand shows high plasma protein binding (PPB = 97.2%) and significant BBB permeability (0.899), traits associated with longer circulation but potential CNS side effects. In contrast, compounds like Salidroside and beta-Glucogallin demonstrate moderate PPB (61.5% and 51.9%) and very low BBB penetration, ideal for targeting peripheral sites like EGFR. Natural compounds generally show higher unbound fractions (Fu), suggesting improved distribution. For metabolism, native ligand shows interactions with multiple CYP450 enzymes, increasing the risk of metabolic liability. Conversely, most plant derivatives, including Pentagalloyl glucose and Geraniin, exhibit minimal CYP inhibition, reducing metabolic interaction risk. Salidroside and beta-Glucogallin again emerge as promising molecules with safer distribution and metabolic profiles compared to native ligand.

Excretion and toxicity results (Table 8) reveal that native ligand has a shorter half-life (T1/2 = 0.94 h) and moderate clearance (CL = 4.13 mL/min/kg). In comparison, Geraniin and Pentagalloyl glucose show longer half-lives (6.79 h and 3.96 h), which could enhance therapeutic duration. Toxicity markers indicate that native ligand has a higher human hepatotoxicity (H-HT = 0.91) and DILI risk (0.94), raising concerns. In contrast, beta-Glucogallin, Luteolin-7-O-rutinoside, and Salidroside display low hepatotoxicity and minimal DILI potential. Additionally, beta-Glucogallin exhibits the lowest rat oral acute toxicity and eye irritation risk. Carcinogenicity and skin sensitization are minimal in several plant compounds, with Pentagalloyl glucose and Salidroside being non-carcinogenic. Collectively, these findings highlight the superior safety profiles of many natural candidates over native ligand, positioning them as safer alternatives for long-term use.

Environmental toxicity is vital for sustainable drug development (Table 9). Native ligand exhibits higher bioaccumulation (BCF = 1.74), indicating potential environmental persistence. In contrast, most natural compounds have lower BCF values—Geraniin and beta-Glucogallin being the least bioaccumulative. Acute aquatic toxicity parameters (IGC50, LC50FM, LC50DM) for native ligand are moderate to high, but several derivatives such as Pentagalloyl glucose and Procyanidin B2 3-O-gallate show comparable or reduced aquatic toxicity. Salidroside, despite moderate aquatic toxicity, demonstrates minimal BCF, making it an environmentally friendly candidate. These data suggest that many plant-based molecules offer better environmental compatibility than native ligand, reducing ecological risks associated with pharmaceutical residues.

Table 4. Physicochemical properties of selected derivatives

Compounds	MW	Volume	Dense	nHA	nHD	nRot	nRing	TPSA	logS	logP
Native Ligand	407.16	431.7665	0.94301	5	2	6	5	71.18	-4.51979	4.281666
3,5-Di-O-caffeoylquinic acid	530.14	509.0644	1.041401	12	6	10	3	200.28	-3.83564	1.700778
beta-Glucogallin	332.07	293.6478	1.130845	10	7	4	2	177.14	-1.09457	-1.23267
Geraniin	952.08	827.9271	1.149956	27	14	3	9	450.25	-3.44192	-1.25747
Luteolin-7-O-rutinoside	610.15	552.3177	1.104708	16	10	7	5	269.43	-2.80468	-0.20424
Oleanolic acid 3-O-glucoside	618.41	644.9221	0.958891	8	5	4	6	136.68	-4.21268	3.357353
Pentagalloyl glucose	940.12	842.1698	1.116307	26	15	16	6	444.18	-3.69952	0.446222
Procyanidin B2 3-O-gallate	730.15	687.073	1.062696	16	12	6	7	287.52	-4.72818	1.611179
Salidroside	300.12	287.2095	1.044951	7	5	5	2	119.61	-1.35823	-0.57356

Table 5. Drug-likeness properties of designed derivatives

Compounds	QED	NP Score	Lipinski Rule	Pfizer Rule	GSKRule	GoldenTriangle	Chelator Rule
Native Ligand	0.378	-0.332	0	1	1	0	0
3,5-Di-O-caffeoylquinic acid	0.129	1.294	1	0	1	1	1
beta-Glucogallin	0.236	2.039	0	0	0	0	1

Geraniin	0.049	1.516	1	0	1	1	1
Luteolin-7-O-rutinoside	0.125	1.718	1	0	1	1	1
Oleanolic acid 3-O-glucoside	0.218	3.166	0	0	1	1	0
Pentagalloyl glucose	0.051	0.617	1	0	1	1	1
Procyanidin B2 3-O-gallate	0.09	1.648	1	0	1	1	1
Salidroside	0.461	1.913	0	0	0	0	0

Table 6. Absorption parameter of selected compounds

Compounds	Caco-2 Permeability	MDCK Permeability	Pgp-inhibitor	Pgp-substrate	HIA	F20%	F30%	F50%
Native Ligand	-4.58617	-4.91909	0.911321	0.005203	9.54E-06	0.000438	0.097472	0.370549
3,5-Di-O-caffeoylquinic acid	-6.3104	-5.17535	0.012005	0.01178	0.177099	0.999987	0.999997	0.999999
beta-Glucogallin	-6.43934	-5.10732	3.40E-05	0.036917	0.046665	0.62458	0.993436	0.97752
Geraniin	-7.17547	-4.92208	9.35E-12	0.00087	0.024233	0.799404	0.979921	0.999722
Luteolin-7-O-rutinoside	-6.7156	-5.03995	2.30E-07	0.577169	0.949759	0.925576	0.999797	0.999857
Oleanolic acid 3-O-glucoside	-5.65535	-5.1073	0.002246	0.001136	0.004817	0.149527	0.367533	0.958809
Pentagalloyl glucose	-8.02009	-4.59086	3.68E-07	1.62E-06	0	0.999913	0.999563	0.999999
Procyanidin B2 3-O-gallate	-7.60333	-4.79234	2.95E-06	0.018163	0.000195	0.999927	0.999999	1
Salidroside	-6.49754	-5.10257	0.000404	0.718975	0.925774	0.511553	0.93326	0.990222

Table 7. Distribution and metabolism parameter of selected molecules

Compounds	Distribution				Metabolism									
					CYP1A2		CYP2C19		CYP2C9		CYP2D6		CYP3A4	
	PPB %	VD	BBB	Fu	Inhibitor	Substrate	Inhibitor	Substrate	Inhibitor	Substrate	Inhibitor	Substrate	Inhibitor	Substrate
Native Ligand	97.1992	0.091418	0.898616	2.590976	0.997226	0.000267	0.627591	2.14E-06	0.960957	0.608994	0.019331	0.936086	0.008908	0.003544
3,5-Di-O-caffeoylquinic acid	74.27631	0.845307	6.20E-05	31.07112	4.68E-05	1.14E-11	0.000131	4.44E-09	2.03E-05	1.92E-08	2.69E-05	1.81E-09	0.000161	2.61E-07
beta-Glucogallin	51.94361	-0.43234	0.014107	48.10594	9.73E-09	1.25E-06	2.67E-10	2.77E-09	3.14E-05	3.18E-07	4.46E-08	1.61E-11	0.004582	1.76E-08
Geraniin	73.10837	0.019778	2.84E-07	21.45141	2.14E-11	2.03E-11	7.08E-15	6.01E-16	0.002594	0.022318	1.57E-15	3.14E-14	0.000818	2.39E-17
Luteolin-7-O-rutinoside	79.38117	-0.06624	5.35E-05	19.31586	1.21E-05	2.50E-07	3.41E-09	3.09E-10	4.57E-08	2.25E-08	2.27E-07	2.77E-07	0.001574	1.92E-07

Oleanolic acid 3-O-glucoside	86.31084	-0.5648	0.004694	9.118204	1.15E-14	3.59E-08	1.55E-06	0.160664	0.032948	0.001901	4.47E-11	2.08E-09	4.79E-05	0.387681
Pentagalloyl glucose	72.08147	-0.18526	2.05E-08	15.42953	4.41E-14	1.03E-19	3.25E-08	4.28E-25	0.996677	4.37E-24	4.17E-17	0	1	4.85E-15
Procyanidin B2 3-O-gallate	90.43642	-0.08775	0.000146	11.81428	1.35E-09	0.005679	8.94E-05	1.35E-05	9.45E-05	1.21E-05	8.57E-13	4.03E-19	7.13E-05	3.48E-10
Salidroside	61.48026	-0.31045	0.215823	37.74579	0.0002	0.000282	0.000104	4.84E-05	0.01129	0.000387	0.002976	0.105142	0.010104	0.015117

Table 8. Excretion and Toxicity parameters of selected compounds

Compounds	Excretion		Toxicity									
	CL-plasma	T1/2	H-HT	DILI	Ames Toxicity	Rat Oral Acute Toxicity	FDAMDD	Skin Sensitization	Carcinogenicity	Eye Corrosion	Eye Irritation	Respiratory Toxicity
Native Ligand	4.126864	0.943475	0.912443	0.941637	0.339517	0.345748	0.649427	0.606516	0.215791	5.70E-06	0.451973	0.139994
3,5-Di-O-caffeoylquinic acid	8.529292	2.125312	0.442877	0.383517	0.589438	0.296728	0.952366	0.999249	0.179829	0.000175	0.146278	0.125575
beta-Glucogallin	3.442103	3.216254	0.284081	0.941776	0.929461	0.031762	0.054055	0.999976	0.26537	0.000844	0.832406	0.017694
Geraniin	2.827989	6.798095	0.727279	0.999726	0.997466	0.293301	0.985456	1	0.920056	9.43E-09	0.147463	0.00066
Luteolin-7-O-rutinoside	1.547739	5.024143	0.304035	0.796593	0.811954	0.018622	0.042434	0.936664	0.107949	3.25E-07	0.322165	0.002625
Oleanolic acid 3-O-glucoside	0.85621	1.785285	0.800224	0.890555	0.606336	0.080402	0.055432	0.992305	0.783123	7.31E-05	0.06112	0.183708
Pentagalloyl glucose	6.890484	3.962382	0.00708	0.996347	0.741346	0.028149	0.952092	1	0.038747	1.16E-05	0.986932	0.009588
Procyanidin B2 3-O-gallate	7.416264	4.268013	0.370049	0.759942	0.816889	0.573347	0.981624	1	0.049464	1.98E-06	0.947332	0.746492

Salidroside	3.28087 6	2.104587	0.48025 2	0.34456 3	0.65363 1	0.02250 2	0.012426	0.965046	0.111709	0.002146	0.789604	0.008728

Table 9. Environmental toxicity profile of designed molecules

Compounds	BCF	IGC50	LC50FM	LC50DM
Native Ligand	1.74498	4.316715	4.879549	4.918118
3,5-Di-O-caffeoylquinic acid	0.591311	3.601962	4.689656	4.983431
beta-Glucogallin	0.178403	2.577124	3.348462	3.999531
Geraniin	-0.05914	3.232598	4.168432	4.096771
Luteolin-7-O-rutinoside	0.375347	2.788211	3.590672	4.422757
Oleanolic acid 3-O-glucoside	1.380894	3.870243	4.734317	5.532188
Pentagalloyl glucose	0.281061	3.592419	4.416571	4.446641
Procyanidin B2 3-O-gallate	0.971416	3.826815	4.438632	4.988047
Salidroside	0.326215	2.181263	3.065471	3.750632

Table 10. ADMET radar of all selected derivative and native ligand.

Native Ligand

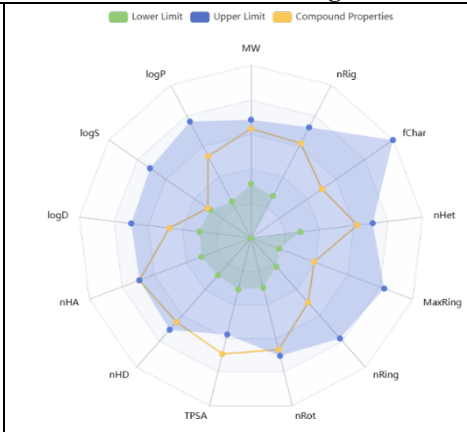

3,5-Di-O-caffeoylquinic acid

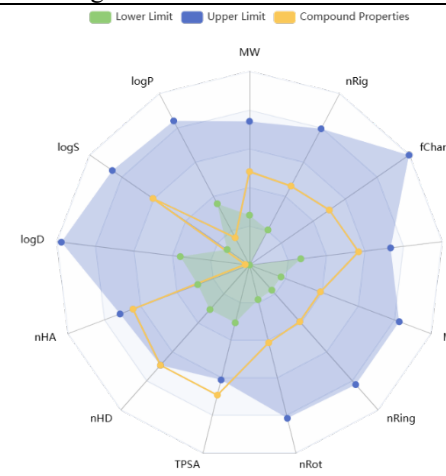

beta-Glucogallin

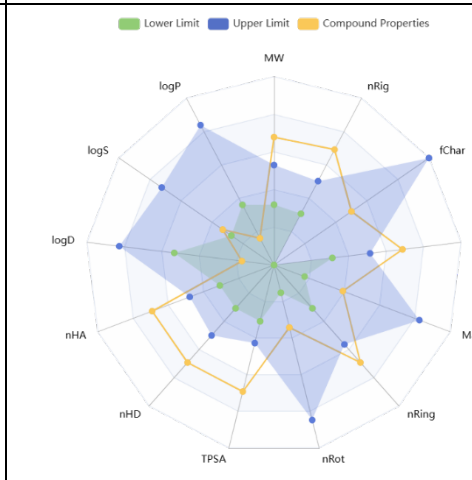

Geraniin

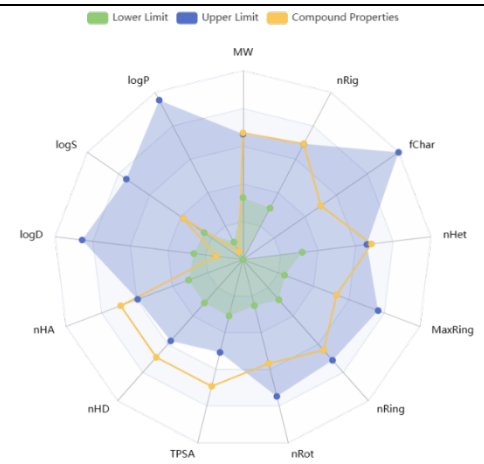

Luteolin-7-O-rutinoside

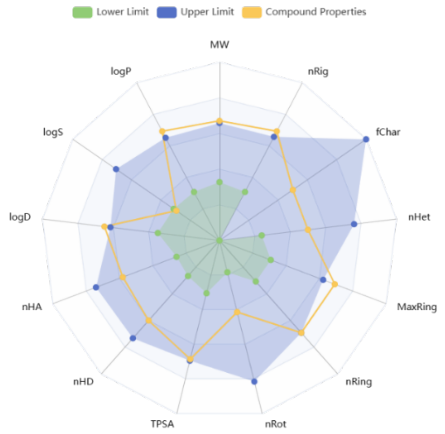

Oleanolic acid 3-O-glucoside

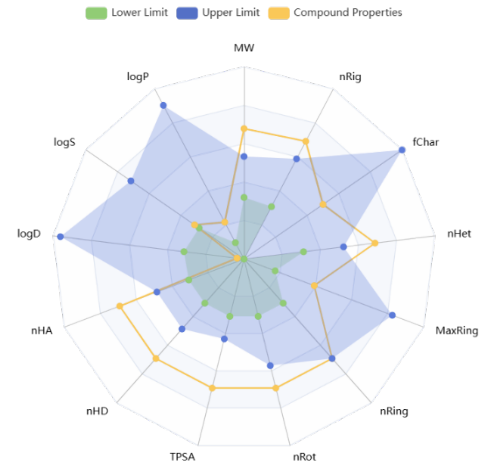

Pentagalloyl glucose

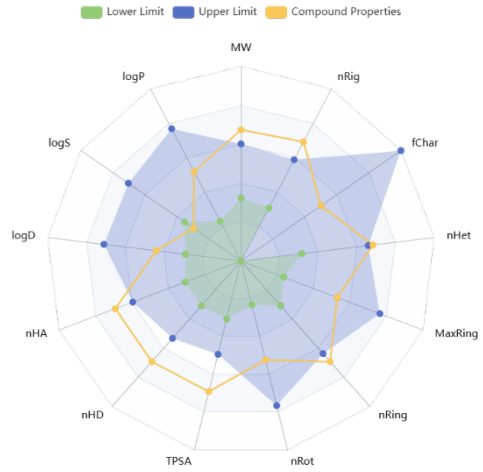

Procyanidin B2 3-O-gallate

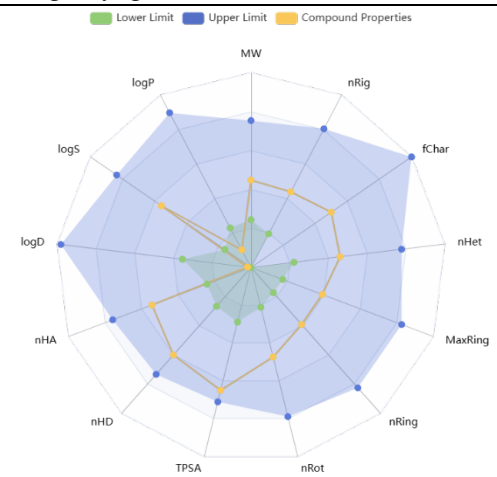

Salidroside

CONCLUSION

In conclusion, the hydroalcoholic extract of *Verbascum coromandelianum* demonstrated a promising phytopharmacological profile supported by organoleptic, physicochemical, phytochemical, and advanced analytical assessments. The extract showed acceptable physicochemical parameters, including stable pH, absence of heavy metals, and optimal ash and extractive values, ensuring both purity and safety. Preliminary phytochemical screening confirmed the abundance of polyphenols and flavonoids, alongside tannins, steroids, and fatty acids,

which are well recognized for their therapeutic potential. Microbial analysis further validated its safety, confirming the absence of pathogenic organisms and establishing suitability for pharmacological development. LC-HRMS profiling revealed a diverse array of bioactive compounds, including salidroside, luteolin-7-O-rutinoside, caffeoylquinic acids, oleanolic acid glycoside, procyanidins, gallotannins, and ellagitannins. These metabolites are widely documented for their antioxidant, anti-inflammatory, hepatoprotective, antidiabetic, cardioprotective, and anticancer properties, providing a strong chemical rationale for the plant's traditional medicinal applications. Molecular docking studies reinforced this potential, with key phytoconstituents such as geraniin, oleanolic acid 3-O-glucoside, pentagalloyl glucose, and luteolin-7-O-rutinoside exhibiting stronger binding affinities toward EGFR than the native ligand. Their ability to form multiple hydrogen bonds, electrostatic, and hydrophobic interactions with crucial residues indicates potential anticancer activity through EGFR inhibition. Complementary ADMET predictions highlighted favorable drug-likeness, bioavailability, lower toxicity, and reduced metabolic liabilities for several plant-derived molecules, particularly salidroside and beta-glucogallin. Additionally, environmental safety assessments suggested lower bioaccumulation and ecological toxicity compared to the native ligand, underscoring their sustainability advantages. Overall, the findings establish *Verbascum coromandelianum* as a rich source of bioactive phytoconstituents with significant therapeutic promise, particularly in oxidative stress-related and cancer management. Further in vitro and in vivo validation, along with formulation development, is warranted to translate these leads into potential drug candidates...

.

REFERENCES

1. Mansour HM, Fawzy HM, El-Khatib AS, Khattab MM. Repurposed anti-cancer epidermal growth factor receptor inhibitors: mechanisms of neuroprotective effects in Alzheimer's disease. Neural Regen Res. 2022; 17:1913–8.
2. Xu H, Zong H, Ma C, Ming X, Shang M, Li K, et al. Epidermal growth factor receptor in glioblastoma (review). Oncol Lett. 2017; 14(1):512–6.
3. Hatil AC, Cicek E, Oyken M, Erson-Bensan AE. EGFR (epidermal growth factor receptor). Atlas Genet Cytogenet Oncol Haematol. 2020; 24(9):325–32.
4. Wee P, Wang Z. Epidermal growth factor receptor cell proliferation signaling pathways. Cancers (Basel). 2017 May 17; 9(5):52.
5. Nurisyah, Ramadhan DSF, Dewi R, Asikin A, Daswi DR, Adam A, et al. Targeting EGFR allosteric site with marine natural products of Clathria sp.: a computational approach. Curr Res Struct Biol. 2024; 7:100083.
6. Zang H, Qian G, Arbiser J, Owonikoko TK, Ramalingam SS, Fan S, et al. Overcoming acquired resistance of EGFR-mutant NSCLC cells to the third-generation EGFR inhibitor osimertinib with the natural product honokiol. Mol Oncol. 2020; 14(4):882–95.
7. Agarwal SM, Nandekar P, Saini R. Computational identification of natural product inhibitors against EGFR double mutant (T790M/L858R) by integrating ADMET, machine learning, molecular docking and dynamics approaches. RSC Adv. 2022; 12(26):16779–89.
8. Abdallah MS, Mustafa M, Nallappan MA, Choi S, Paik JH, Rusea G. Determination of phenolics and flavonoids of some useful medicinal plants and bioassay-guided fractionation of Sclerocarya birrea stem bark extract and their efficacy against Salmonella typhi. Front Chem. 2021; 9:675648.
9. Lima GS, Lima NM, Roque JV, de Aguiar DVA, Oliveira JVA, dos Santos GF, et al. LC-HRMS/MS-based metabolomics approaches applied to the detection of antifungal compounds and metabolic dynamic assessment of Orchidaceae. Molecules. 2022; 27(22):7839.
10. Luca SV, Zengin G, Sinan KI, Korona-Glowniak I, Minceva M, Skalicka-Woźniak K, et al. Value-added compounds with antimicrobial, antioxidant, and enzyme-inhibitory effects from post-distillation and post-supercritical CO_2 extraction by-products of rosemary. Antioxidants (Basel). 2023; 12(2):327.
11. La Basy L, Hertiani T, Murwanti R, Damayanti E. Investigation of COX-2 inhibition of Laportea decumana (Roxb.) Wedd. extract to support its analgesic potential. J Ethnopharmacol. 2024; 318:117105.
12. Tamboli AS, Tayade SD. In-depth investigation of berberine and tropane through computational screening as possible DPP-IV inhibitors for the treatment of T2DM. J Pharm Sci Comput Chem. 2025;1(1):1–11.
13. Siddiqui FA, Makhloufi R, Hojjati M, El-Sayed MS, Eman K. Computational exploration of quinine and mefloquine as potential anti-malarial agents. J Pharm Sci Comput Chem. 2025; 1(2):106–15.
14. Ahmed SA, Tabassum PS, Falak SA, Vikhar A, Ahmad D, Shaikh S. Molecular docking and network pharmacology: investigating Vitis vinifera phytoconstituents as multi-target therapeutic agents against breast cancer. J Pharm Sci Comput Chem. 2025; 1(2):116–34.
15. Jadhav SS, Dighe PR, Kumbhare MR. Synthesis, in vitro evaluation, and molecular docking studies of novel pyrazoline derivatives as promising bioactive molecules. J Pharm Sci Comput Chem. 2025;1(3):1–12.
16. Sharma V, Janmeda P. Extraction, isolation and identification of flavonoid from Euphorbia neriifolia leaves. Arab J Chem. 2017; 10(4):509–14.

17. Nickavar B, Mojab F, Javidnia K, Roodgar Amoli MA. Chemical composition of the fixed and volatile oils of Nigella sativa L. from Iran. Z Naturforsch C J Biosci. 2003; 58(9–10):629–31.
18. Talreja T, Kumar M, Goswami A, Gahlot G, Jinger AK, Sharma T. HPLC analysis of saponins in Achyranthes aspera and Cissus quadrangularis. Pharma Innov J. 2017; 6(1):76–9.
19. Chinala KM, Chaithanya A, Sawrov M, Sahithi A, Achyuth C. Phytochemical and antimicrobial evaluation of Laurus nobilis leaves against acne- and dandruff-causing microorganisms. J Pharm Sci Comput Chem. 2025; 1(1):50–7.
20. Khandelwal KR. Practical pharmacognosy: techniques and experiments. 20th ed. Pune: Nirali Prakashan; 2005. p. 150–153.
21. Mukherjee PK. Quality control of herbal drugs: an approach to evaluation of botanicals. New Delhi: Business Horizons; 2002. p. 1–800.
22. Singh M, Tamboli ET, Kamal YT, Ahmad W, Ansari SH, Ahmad S. Quality control and in vitro antioxidant potential of Coriandrum sativum Linn. J Pharm Bioallied Sci. 2015; 7:280–3.
23. Kamal Y, Singh M, Salam S, Ahmad S. Standardization of Unani polyherbal formulation Qurse-e-Hummaz: a comprehensive approach. Drug Dev Ther. 2016; 7(1):39.
24. Chaudhari RN, Khan SL, Chaudhary RS, Jain SP, Siddiqui FA. β-Sitosterol: isolation from Muntingia calabura Linn bark extract, structural elucidation and molecular docking studies as potential inhibitor of SARS-CoV-2 Mpro (COVID-19). Asian J Pharm Clin Res. 2020; 13(5):204–9.
25. Indrayanto G. Recent development of quality control methods for herbal-derived drug preparations. Nat Prod Commun. 2018; 13(12):1599–606.
26. Al-Busaid MM, Akhtar MS, Alam T, Aly Shehata W. Development and evaluation of herbal cream containing curcumin from Curcuma longa. Pharm Pharmacol Int J. 2020;8(5):285–9.
27. Vasincu A, Luca SV, Charalambous C, Neophytou CM, Skalicka-Woźniak K, Miron A. LC-HRMS/MS phytochemical profiling of Vernonia kotschyana: potential involvement of highly oxygenated stigmastane-type saponins in cancer cell viability, apoptosis and intracellular ROS production. S Afr J Bot. 2022; 144:83–91.
28. Luca SV, Minceva M, Gertsch J, Skalicka-Woźniak K. LC-HRMS/MS-based phytochemical profiling of Piper spices: global association of piperamides with endocannabinoid system modulation. Food Res Int. 2021; 141:110132.
29. Kızıltaş H, Bingöl Z, Gören AC, Pinar SM, Alwasel SH, Gülçin İ. LC-HRMS profiling of phytochemicals, antidiabetic, anticholinergic and antioxidant activities of evaporated ethanol extract of Astragalus brachycalyx Fischer. J Chem Metrol. 2021; 15(2):135–51
.